

## Spatial patterns of northeast monsoon rainfall over sub-regions of southern peninsular India and Sri Lanka as revealed through empirical orthogonal function analysis

B. GEETHA and Y. E. A. RAJ

*India Meteorological Department, Chennai – 600 006, India*

*(Received 18 May 2011, Modified 15 April 2013)*

**e mail : geethab67@gmail.com**

**सार** – इस शोध पत्र में अक्टूबर, नवम्बर, दिसम्बर, जनवरी के महीनों में हुई मासिक / ऋतुनिष्ठ वर्षा आँकड़ों पर आधारित इम्पीरिकल ऑर्थोगोनल फंक्शन (EOF) विश्लेषण का उपयोग करते हुए प्रायद्वीपीय भारत और श्रीलंका में पूर्वोत्तर मॉनसून (NEM) वर्षा की आकाशीय परिवर्तितता का अध्ययन किया गया है तथा वर्ष 1900-2006 तक 107 वर्षों की अवधि में अक्टूबर से दिसम्बर तक की ऋतु में जलवायु विज्ञान और भूगोल द्वारा निर्धारित नौ उप-क्षेत्रों में हुई मासिक / ऋतुनिष्ठ वर्षा आँकड़ों का अध्ययन किया गया है। इन नौ उप-क्षेत्रों में हुई मासिक / ऋतुनिष्ठ वर्षा श्रृंखलाएँ ई ओ एफ (EOF) विश्लेषण पर आधारित हैं और प्रत्येक स्थितियों के लिए 2-3 महत्वपूर्ण प्रमुख अवयवों (PCs) की पहचान की गई है। सहसंबंध और समिश्रित तकनीकों का उपयोग करते हुए प्रत्येक प्रमुख अवयव को पूर्वोत्तर मॉनसून से संबंधित भौतिक मोड्स के साथ जोड़ा गया है। प्रथम प्रमुख अवयव (पी सी) से आकाशीय वर्षा वितरण में 49-64 प्रतिशत के अधिकतम अंतर को दर्शाते हुए अक्टूबर से दिसम्बर तक की ऋतु में और सभी चारों महीनों के लिए अलग-अलग पूर्वोत्तर मॉनसून (एन ई एम) की पहचान की गई है। द्वितीय एवं तृतीय प्रमुख अवयवों की पहचान अक्टूबर में (15 प्रतिशत अंतर बताया गया है) पूर्वोत्तर मॉनसून के आगमन के पूर्व सिनॉप्टिक पैमाना प्रणालियों जैसे:- चक्रवातों और अवदाबों (जिसमें 11-20 प्रतिशत का अंतर बताया जाता है) के कारण हुई वर्षा तथा दक्षिण पश्चिमी मॉनसून वर्षा से की गई है। प्रमुख अवयव पूर्वोत्तर मॉनसून सक्रियता को दर्शाते हैं और दक्षिण पश्चिमी मॉनसून मुख्य जलवायु सूचकांक दक्षिणी दोलन सूचकांक के साथ विरोधी प्रकृति को दर्शाता है। प्रमुख अवयवों और महत्वपूर्ण क्षेत्रीय परिसंचरण की विशेषताओं उदाहरणार्थ, 200 हे.पा. स्तर पर उपोष्ण कटक तथा 850 हे.पा. पर भूमध्य रेखीय द्रोणी, का उपयोग दक्षिण पश्चिमी मॉनसून से संबंधित प्रमुख अवयवों और अक्टूबर के दौरान हुई पूर्वोत्तर मॉनसून वर्षा को दर्शाने के लिए किया गया है। इस अध्ययन से यह पता चला है कि आंध्र प्रदेश के उत्तरी तटीय उप खंड को पूर्वोत्तर मॉनसून सक्रियता से फायदा नहीं होता है परन्तु पूर्वोत्तर मॉनसून के आगमन के पूर्व चक्रवातीय विक्षोभों और दक्षिण पश्चिमी मॉनसून के गुजरने के कारण वर्षा होती है।

**ABSTRACT.** The spatial variability of northeast monsoon (NEM) rainfall of peninsular India and Sri Lanka is studied using Empirical Orthogonal Function (EOF) analysis based on monthly / seasonal rainfall data for the months of October, November, December, January and for the season October-December (OND) for the 107 year period of 1900-2006 over nine sub-regions defined for the study based on climatology and geography. Monthly / seasonal rainfall series over these nine sub-regions are subjected to EOF analysis and 2-3 significant Principal Components (PCs) are identified for each case. Each PC is then linked to physical modes known to be associated with NEM using correlation and compositing techniques. For the OND season and for all the four individual months, the first PC explaining maximum variance of 49-64% in the spatial rainfall distribution is identified with the overall NEM strength. The second and the third PCs are identified with rainfall due to passage of synoptic scale systems such as cyclones and depressions (explaining 11-20% variation) and southwest monsoon (SWM) rainfall prior to onset of NEM in October (15% variance explained). PCs representing NEM strength and SWM contribution exhibit contrasting nature of relation with the major climate index Southern Oscillation Index. Relation between the PCs and important regional circulation features, viz., the subtropical ridge at 200 hPa level and the equatorial trough at 850 hPa are used to delineate the PCs associated with SWM and NEM rainfall during October. The study also reveals that the sub-region of north coastal Andhra Pradesh is not

benefitted by the over NEM strength but, receives rainfall due to passage of cyclonic disturbances and SWM prior to NEM onset.

**Key words** – Northeast monsoon, India, Sri Lanka, Empirical orthogonal function, Principal component, Southern oscillation index, Sub tropical ridge, Equatorial trough.

## 1. Introduction

The Indian southwest monsoon (SWM) which affects India during the period June-September is the most important weather event, providing the country with nearly 75% of its annual rainfall. A good number of research works on inter-annual, intra-seasonal and spatial variability of SWM rainfall and its seasonal forecasting have been carried out (Srivastava and Singh (1993), Kondragunta (2001) and Guhathakurtha (2003)). Rao (1976) and Asnani (2005) provide a detailed exposition on SWM and review a large number of research studies on its various aspects. After the withdrawal of SWM from most parts of India in September / October, the southern parts of India experience northeast monsoon (NEM) during October-December. For the state of Tamil Nadu which lies in the rain shadow region during SWM and so receives only modest rainfall, the NEM is the principal rainy season bestowing it with agricultural and hydrological sustenance.

Though NEM is a small scale monsoon confined mainly to parts of southern Indian peninsula, NEM rainfall (NMR) manifests noticeable spatial and temporal variation. In the northern sub-divisions, the rainfall of October is substantial. As the season advances into December, rainfall decreases over the northern region but continues over the south and the east. The east coast of the southern peninsula receives more rainfall than the interior regions. The stretch of coastal Tamil Nadu (CTN) receives nearly 60% of its annual rainfall during this season. Further, the NMR spills over to January of next calendar year in nearly one-third of the years predominantly over CTN (Raj, 2003). The following are the major synoptic scale systems / features associated with the occurrence of NMR: (i) Cyclones and Depressions (CDs), (ii) low pressure areas, (iii) easterly waves and (iv) troughs off Sri Lanka (SL) - Southeast coast of peninsular India. The low pressure systems / waves cited at (i)-(iii) form over Bay of Bengal (BOB) and move towards the peninsula [IMD, 1973 (a&b)].

The characteristics of spatial variation of rainfall and the physical mechanisms that cause such variation are subjects of scientific interest and intrigue. The Empirical Orthogonal Function (EOF) analysis [also referred as Principal Component Analysis (PCA)] is the most popular

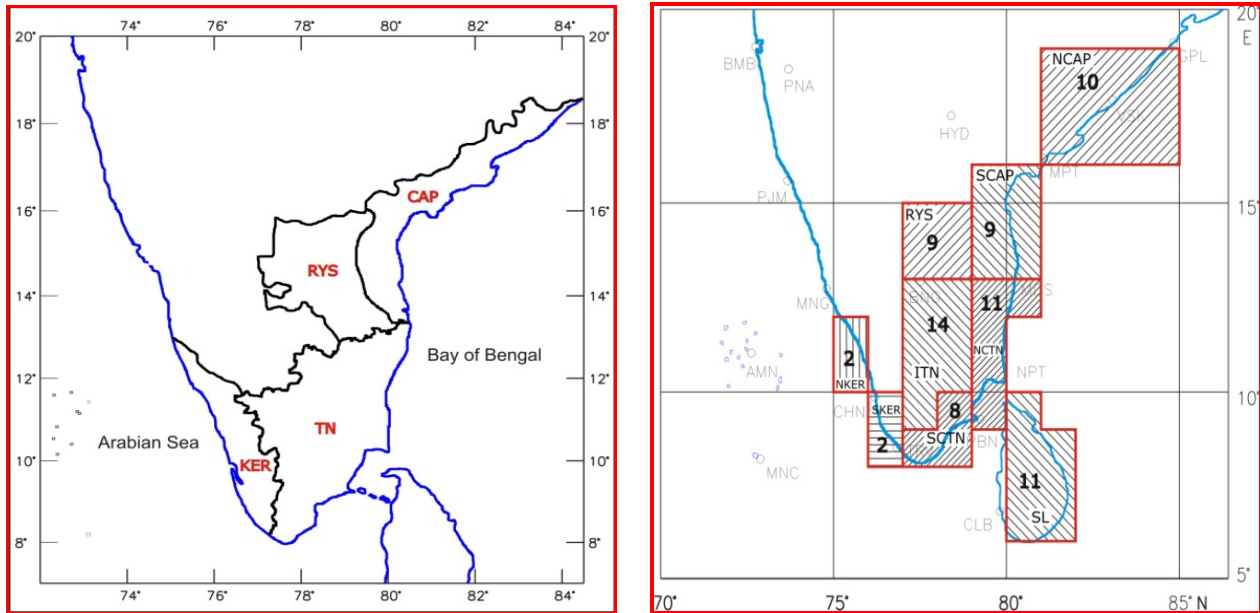
statistical technique employed by the meteorological community to study the spatial patterns of the meteorological parameters and to extract out the components associated with different physical modes from a dataset. The EOF/PCA techniques for meteorological analysis have been described / used in Lorenz (1956), Wilks (2010), Bartzokas *et al.* (1994), Everson *et al.* (1997), Yen and Chen (2000). In the Indian context, this technique has been used to study the variability in SWM rainfall by Bedi and Bindra (1980), Srivastava and Singh (1993), Singh (2004) and Mohapatra *et al.* (2011). Nayagam *et al.* (2009) have used EOF and Wavelet analysis techniques to study the spatial and temporal variabilities of rainfall over peninsular India during the NEM season in relation to SST over Indian, Atlantic and Pacific oceans.

In the present study, the spatial variability of NMR over peninsular India is analysed in detail by employing EOF analysis. The objective is to associate the various empirical modes generated through EOF technique with the physical and synoptic features known to be associated with NEM thereby determining quantitatively the contributions from large and synoptic scale features in causing spatial rainfall variation during the NEM season. The analysis is conducted for the individual months also to understand the intra-seasonal variation of spatial rainfall distribution.

## 2. Data and methodology

### 2.1. NEM sub-regions selected and defined for the study

The four major meteorological sub divisions of southeast peninsular India benefitted by NEM are Coastal Andhra Pradesh (CAP), Rayalaseema (RYS), Tamil Nadu (TN) and Kerala (KER). Table 1(a) presents the normal rainfall of the above four sub-divisions for the months of October, November, December and January, for the NEM season of OND, the annual rainfall and NEM rainfall expressed as percentage of annual rainfall. The NMR contribution is as much as 48% for TN and is 31-32% for CAP and RYS. Though NMR contributes only 16% of annual rainfall of Kerala, the quantum of rainfall received is quite high at nearly 48 cm. These figures testify to the importance of NMR in the annual rainfall climatology of the above four regions.



**Figs. 1(a&b).** (a) Geographical locations of the four meteorological sub-divisions of southern peninsular India and Sri Lanka considered for the present study and (b) the nine sub-regions defined for the study. The number of grid points in each sub-region is indicated inside each

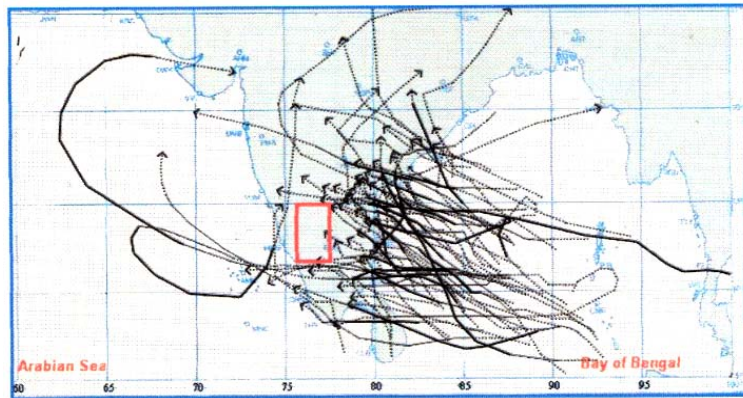


**Fig. 1(c).** Tracks of cyclones and depressions that affected NEM region during OND, 1971-2010. Approximate location of the sub division SIK is marked by a red box

The inter annual variability of NEM rainfall over all the four sub-divisions is high as seen, from the coefficient of variation (CV) of OND rainfall (27-40%). In the intra-seasonal scale, rainfall during November is about half of the October rainfall and that during December is only meagre and is about one-third of that of November over all the three sub-divisions excepting TN. Over TN, November rainfall is as high as that during October and rainfall during December is also considerably high. Sri Lanka, which receives good amount of rainfall throughout the Indian NEM period of OND and the season extending into

January, and is geographically located close to the Indian NEM area is also considered in the study [Fig. 1(a)].

To enable study of spatial rainfall variation in a higher resolution, the four meteorological sub-divisions considered are divided into 8 sub-regions of longitudinal and latitudinal grids based on climatology and geographical factors as shown in Fig. 1(b). Here, these divisions of sub-regions, do not strictly adhere to meteorological / political sub-divisions, but, by and large, represent distinct climatological characteristics of NEM

TABLE 1(a)

## Monthly / seasonal / annual normal rainfall of five southern Indian sub divisions influenced by northeast monsoon

Sub-division		Normal rainfall (mm)						CV (OND) in (%)	OND rainfall as percentage of annual rainfall (%)
Name	Area (sq.km)	Annual	Oct	Nov	Dec	OND	Jan		
CAP	92,906	327.4	193.2	106.6	27.6	327.4	8.3	38.0	32
RYS	67,299	219.2	129.4	66.1	23.7	219.2	3.0	39.6	31
TN	1,35,710	438.2	180.2	170.0	88.0	438.2	17.5	27.1	48
KER	38,951	477.5	290.9	149.5	37.1	477.5	8.5	27.5	16

(Source : India Meteorological Department; based on data of 1951-2000)

OND : October to December, CAP : Coastal Andhra Pradesh, RYS : Rayalaseema,  
TN : Tamil Nadu, KER : Kerala, CV : Coefficient of Variation

TABLE 1(b)

## Rainfall statistics during NEM months / season over the nine sub regions considered for analysis

Month/Season	Parameter	NCAP	SCAP	RYS	NCTN	SCTN	ITN	SKER	NKER	SL
Oct	Mean (mm)	178.1	212.4	121.2	213.7	204.2	182.1	362.0	290.1	248.4
	CV (%)	53	54	53	48	38	37	29	45	32
Nov	Mean (mm)	62.2	203.0	56.3	271.3	197.0	124.7	220.4	157.1	316.8
	CV (%)	110	63	86	53	46	55	50	78	28
Dec	Mean (mm)	8.5	70.9	16.2	137.5	94.9	52.3	57.9	34.2	269.2
	CV (%)	194	107	143	82	78	100	88	132	39
OND	Mean (mm)	248.8	486.3	193.7	622.4	496.1	359.1	640.4	481.4	834.3
	CV (%)	46	39	43	33	29	32	27	41	21
Jan	Mean (mm)	7.3	18.0	4.7	41.5	37.0	17.1	20.2	7.6	198.1
	CV (%)	158	159	192	124	103	144	127	221	42

(Based on 107 year data of 1900-01 to 2006-07)

NEM : Northeast monsoon, NCAP : North Coastal Andhra Pradesh, SCAP : South Coastal Andhra Pradesh,  
RYS : Rayalaseema, NCTN : North Coastal Tamil Nadu, SCTN : South Coastal Tamil Nadu,  
ITN : Interior Tamil Nadu, SKER : South Kerala, NKER : North Kerala, SL : Sri Lanka,  
SD : Standard Deviation, CV : Coefficient of variation

activity over the respective areas. The neighbouring Sri Lanka (SL) region is included as the 9<sup>th</sup> sub-region. Thus, nine sub-regions, namely, NCAP, SCAP, RYS, NCTN, SCTN, ITN, NKER, SKER (N-North, S-South and I-Interior) and SL [Fig. 1(b)] are defined to distinctly represent various geographic areas of NEM region and to bring out specific spatial patterns of rainfall in monthly / seasonal scales.

The sub-division of South Interior Karnataka (SIK) in peninsular India, which is also benefitted by the NEM receives 70% of its OND rainfall during the month of October itself (15 cm out of 21 cm) and mainly from the SWM rain spells prior to the onset of NEM. CDs are the major synoptic systems during NEM season and the tracks of these do not generally penetrate into the SIK region.

Fig. 1(c) presents the tracks of CDs during the period OND, 1971-2010 that crossed TN / CAP and penetrated further inland. The location of the sub division of SIK is indicated by a red box which is devoid of CD tracks save for a few that dissipated over this region. In fact, during the period 1971-2010, 139 CDs formed over BOB out of which 22 and 41 crossed TN and CAP respectively, but, only 4 dissipated over SIK. Considering all these facts, the sub-division of SIK and its rainfall are not included in the present analysis.

## 2.2. Basic rainfall data

The basic data used for the study is 1° longitudinal × 1° latitudinal gridded gauge rainfall data of 107 years for the period 1900-2006 downloaded

TABLE 2

Inter CCs between monthly mean rainfall of the nine sub-regions during the northeast monsoon months of Oct- Jan and Season (OND)

Month / Season	Sub region	NCAP	SCAP	RYS	NCTN	SCTN	ITN	SKER	NKER	SL
Oct	NCAP	1.00								
	SCAP	0.45***	1.00							
	RYS	0.38***	0.67***	1.00						
	NCTN	0.07	0.73***	0.51***	1.00					
	SCTN	-0.18#	0.35***	0.25**	0.56***	1.00				
	ITN	0.12	0.60***	0.70***	0.72***	0.54***	1.00			
	SKER	-0.02	0.39***	0.38***	0.45***	0.73***	0.58***	1.00		
	NKER	0.10	0.35***	0.27**	0.30**	0.33***	0.39***	0.54***	1.00	
	SL	-0.09	0.38***	0.26**	0.58***	0.69***	0.54***	0.54***	0.21*	1.00
	Nov	NCAP	1.00							
SCAP		0.45***	1.00							
RYS		0.47***	0.78***	1.00						
NCTN		0.09	0.66***	0.42***	1.00					
SCTN		0.15	0.50***	0.33***	0.67***	1.00				
ITN		0.33***	0.76***	0.71***	0.78***	0.76***	1.00			
SKER		0.22*	0.51***	0.44***	0.60***	0.79***	0.74***	1.00		
NKER		0.30**	0.48***	0.47***	0.45***	0.56***	0.59***	0.56***	1.00	
SL		-0.06	0.34***	0.13	0.64***	0.67***	0.54***	0.51***	0.32***	1.00
Dec		NCAP	1.00							
	SCAP	0.19*	1.00							
	RYS	0.16#	0.83***	1.00						
	NCTN	0.01	0.70***	0.62***	1.00					
	SCTN	-0.02	0.46***	0.36***	0.75***	1.00				
	ITN	0.01	0.74***	0.65***	0.85***	0.78***	1.00			
	SKER	0.09	0.61***	0.55***	0.70***	0.78***	0.82***	1.00		
	NKER	0.09	0.59***	0.46***	0.51***	0.54***	0.67***	0.74***	1.00	
	SL	-0.02	0.13	0.06	0.49***	0.54***	0.41***	0.33***	0.16#	1.00
	OND	NCAP	1.00							
SCAP		0.32***	1.00							
RYS		0.30**	0.72***	1.00						
NCTN		0.02	0.72***	0.49***	1.00					
SCTN		-0.01	0.45***	0.28**	0.68***	1.00				
ITN		0.11	0.69***	0.71***	0.73***	0.66***	1.00			
SKER		0.07	0.52***	0.43***	0.60***	0.70***	0.72***	1.00		
NKER		0.09	0.35***	0.28**	0.32***	0.33***	0.39***	0.49***	1.00	
SL		-0.05	0.35***	0.21*	0.62***	0.64***	0.50***	0.44***	0.14	1.00
Jan		NCAP	1.00							
	SCAP	0.34***	1.00							
	RYS	0.37***	0.85***	1.00						
	NCTN	0.19*	0.61***	0.60***	1.00					
	SCTN	0.21*	0.42***	0.44***	0.77***	1.00				
	ITN	0.21*	0.56***	0.66***	0.81***	0.82***	1.00			
	SKER	0.33***	0.37***	0.36***	0.47***	0.69***	0.65***	1.00		
	NKER	0.07	0.56***	0.56***	0.77***	0.66***	0.70***	0.35***	1.00	
	SL	0.05	0.14	0.07	0.41***	0.42***	0.32***	0.28**	0.27**	1.00

\*\*\*, \*\*, \*, #: significant at 0.1%, 1%, 5% and 10% level respectively,  
 (based on 107 year data, 1900-01 to 2006-07)  
 Abbreviations : As in Tables 1 (a&b)

from the website of JISAO, a cooperative institution of NOAA and University of Washington (<http://jisao.washington.edu/>). From this dataset, rainfall series are generated for this study as detailed below.

Areal average of the  $1^\circ \times 1^\circ$  monthly mean rainfall data of October, November, December and January (of the subsequent year) for the period 1900-2006 computed over the land area of each sub-region is taken to represent the monthly rainfall series of each of the nine sub-regions defined [Fig. 1(b)]. The seasonal OND rainfall series for each sub-region is also generated from the monthly data

### 2.3. Other datasets used

The following data representing various physical features known to be associated with NMR are also used for physical interpretations of the empirical modes obtained through EOF analysis.

(i) Dates of onset and withdrawal of NEM over CTN during the period 1901-2006 [(Raj (2003) and Geetha (2012)].

(ii) Southern Oscillation Index (SOI) during the months of October – January for the period 1901-2006 downloaded from the website of Australian Bureau of Meteorology.

(iii) Latitudinal positions of the sub tropical ridge at 200 hPa level over the central Indian longitude of  $78.5^\circ\text{E}$  [STR200] during the months of October – January for the period 1950-2006 derived from the NCEP reanalysis zonal wind datasets.

(iv) Tracks of CDs over specific areas of the North Indian Ocean during different months and seasons taken from the Cyclone eAtlas – IMD software (IMD, 2008a).

(v) The number of days of CDs during various months / season during 1901-2006 generated from CWCDSTAT software developed at RMC, Chennai (IMD, 2008b).

(vi) NCEP monthly composite datasets.

## 3. Results and discussion

### 3.1. Statistical parameters of rainfall series of the nine sub regions

Table 1(b) presents the mean and CV of each of the 9 sub-regional rainfall series for various months and the NEM season. As seen, there is substantial spatial variation of OND rainfall from 194 mm (RYS) to 834 mm

(SL). The spatial variation of monthly rainfall is 121 mm (RYS) – 362 mm (SKER) for October, 56 mm (RYS) – 317 mm (SL) for November, 9 mm (NCAP) – 269 mm (SL) for December and 5 mm (RYS) – 198 mm (SL) for January. The CV of OND varies from 21 to 46% and is maximum for the sub-region of NCAP. The CVs of individual months are higher than the seasonal values and the monthly CVs generally increase from October to January.

### 3.2. Inter CC matrix

We begin the analysis by computing the inter correlation coefficients (CCs) amongst the time series of 9 sub-regional rainfall of 107 year period, 1900-2006. The CC matrices generated for the individual months and season are presented in Table 2. The level of significance (LS) of the CCs are also indicated. It can be seen that, by and large, there is a high degree of correlation amongst the monthly / seasonal rainfall series of pairs of sub-regions. However, the rainfall over NCAP is seen to be related to that over SCAP and RYS but is not strongly associated with the rainfall over the other sub-regions save for the significant CCs between NCAP and ITN during November and between NCAP and SKER during January. Generally, the CCs are found to be higher between the rainfall time series of collocated regions and decrease when the regions are located apart.

### 3.3. EOF analysis

Next, the  $107 \times 9$  matrix of rainfall anomalies is subjected to EOF analysis by diagonalising the  $9 \times 9$  covariance matrix. Here, the covariance matrix rather than correlation matrix is used for EOF analysis since the variables considered, viz., rainfall series, are like variables possessing the same unit. Further, the covariance matrix gives due weightage to the quantum of rainfall variation than the CC matrix (Wilks, 2010). The analysis has yielded 9 new decomposed data series called the principal components (PCs) which are mutually orthogonal / independent. Each PC is associated with an eigen value of the covariance matrix which is real and positive and further, the eigen value provides a measure of the variance explained (VE) by the respective PC. Each eigen value is also associated with an eigen vector which contains elements called loadings. Each eigen vector element can be plotted on a map at the same location as its corresponding data value for analysis. In the present case, each eigen vector contains nine elements associated with each of the nine sub-regions. The loadings plotted on a map can be analysed spatially. Such a map indicates the geographic distribution of loadings which help us to identify simultaneous data anomalies represented by PCs. The eigen vector pointing towards maximum variability in

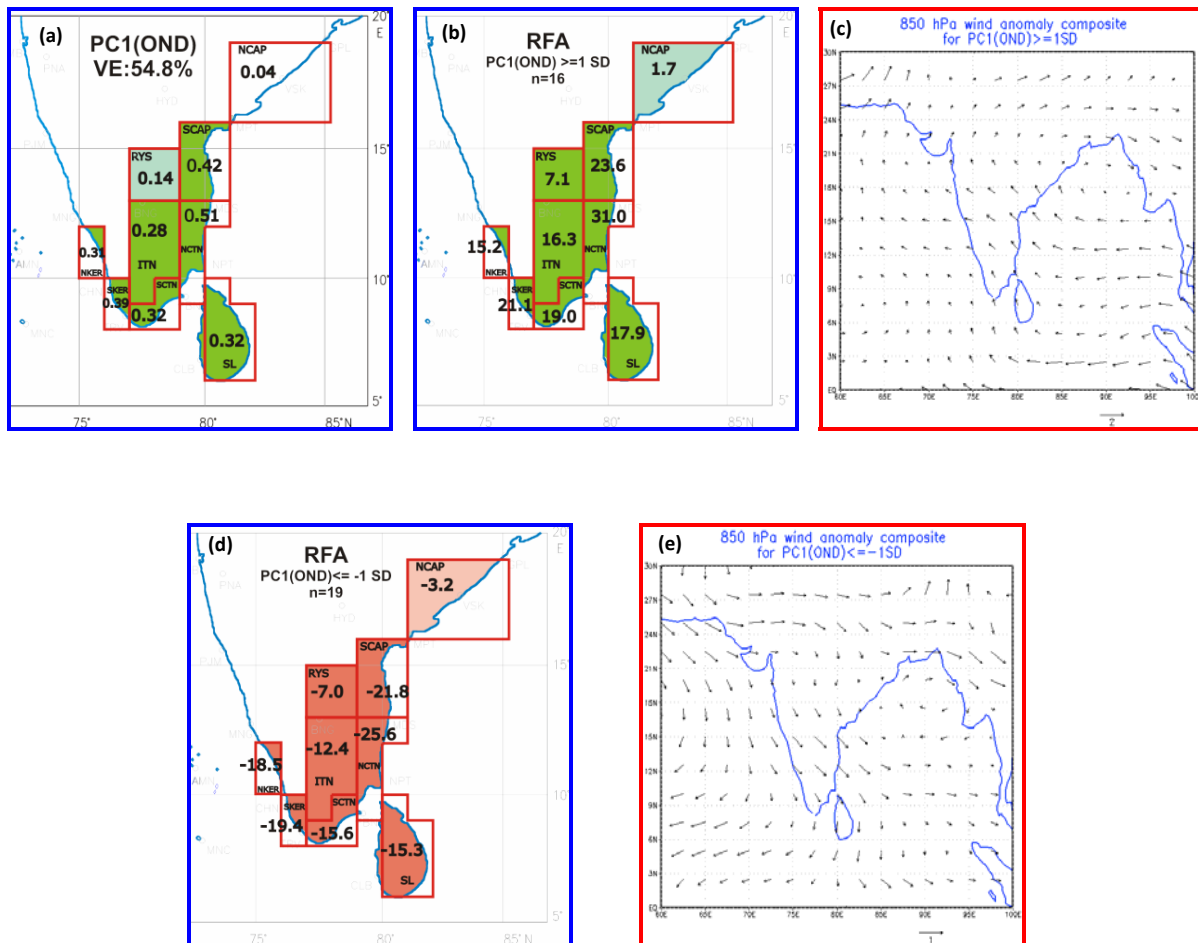


**Fig. 2(i) (a-e).** (a) Spatial loadings of PC1 (OND) (Positive values are shaded in green and negative values in red (absolute values of loadings  $\geq 0.2$  are shaded in dark green/red and  $0.1 \leq \text{absolute value of loadings} < 0.2$  shaded in light green / red); (b&d) Mean composited RFA (OND) (in cm) over the 9 sub-regions during years when PC1 (OND) deviated by 1SD of PC1(OND) (Positive values are shaded in green and negative values in red (absolute values of rainfall anomalies (RFA)  $\geq 5$ cm are shaded in dark green/red and  $1 \text{ cm} \leq \text{absolute values of RFA} < 5$  cm are shaded in light green / red; n: No. of years) and (c&e) Low level (850 hPa) wind anomaly composites during years when PC1 (OND) deviated by 1SD of PC1(OND) (based on NCEP monthly composites, 1950-2006)

the dataset is the first principal component (PC1), the one pointing towards the next highest variance explained is the second PC (PC2) and so on (Wilks, 2010). Reference to Krishnamurthy and Sen (1986) has been made for developing programs written in FORTRAN language to carry out the computations. The results obtained were cross-checked with a standard statistical package - XLSTAT 2010.

The PCs obtained for each month and OND season are tested for significance using Kaiser-Guttman Rule as modified by Jolliffe (Wilks, 2010). According to this rule, PCs with eigen value greater than 0.7 times the average eigen value have to be retained and the other PCs are to be discarded.

The spatial loadings of significant PCs for the season as well as for individual months are plotted and matched with the spatial rainfall distribution patterns associated with various significant PCs. Rainfall anomaly (RFA) maps depicting spatial rainfall patterns obtained from composited RFAs for the concerned months / season during years when the corresponding PC is deviated by more than the respective standard deviation (SD), *i.e.*,  $\pm 1$ SD, are matched with the patterns of spatial loadings for each PC. For bringing out the contributions from physical features, *e.g.*, CDs, the RFAs are matched with the patterns in the composited tracks of CDs during the corresponding years. Such an analysis based on the extreme values of PCs on both the sides is capable of bringing out the relation between the considered PC and

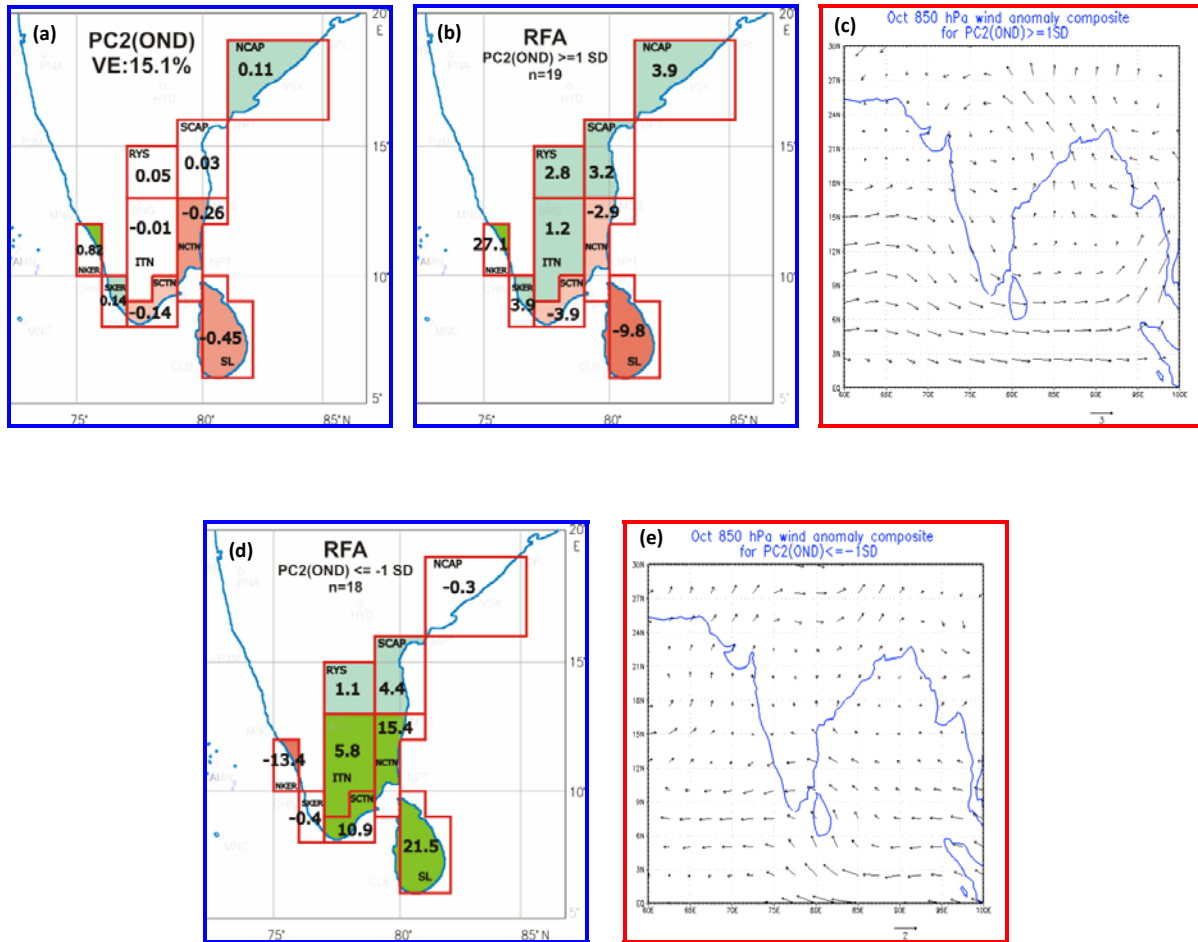


**Fig. 2(ii) (a-e).** (a) Spatial loadings of PC2(OND) and (b-e) mean composited RFA(OND) (in cm) over the 9 sub-regions along with October 850 hPa wind anomaly composites during years when PC2(OND) deviated by 1SD of PC2(OND) (RFA, n & colour codes: as in [Fig. 2(i)]

the associated physical feature, should the relation exist and be clearly defined. Further, correlation and conditional means (CM) analysis are employed to establish physical links between the PCs and NEM features such as dates of onset / withdrawal, relation with SOI and latitudinal location of STR200 known to be associated with NEM activity.

In the forthcoming sections, we present the results of the PCA carried out for the rainfall time series of the nine sub-regions for the season as well as for individual months. Regarding interpretation of signs of loadings, it is reiterated that a positive loading corresponds to positive (negative) contribution by the corresponding PC if the RFA is positive (negative). A negative loading contributes negatively when the RFA is positive but positively when the anomaly is negative.

### 3.3.1. PCA of seasonal (OND) rainfall

The PCA on OND rainfall was carried out as elucidated in the previous section. For the season (OND), the first three PCs are significant which explain 54.8%, 15.1% and 11.1% variance respectively and together they explain 81.0% variance in the dataset. The spatial loadings of these three PCs are presented in Figs. [2(i)a, 2(ii)a & 2(iii)a] respectively.

As shown, all the loadings of PC1, except that of NCAP (0.04) are appreciably positive which implies that the signs of contribution towards this mode are the same as the signs of individual anomalies. The sub-regions of NCTN, SCAP and SKER are more strongly associated with this mode than the other sub-regions. The sub-region of NCAP does not contribute significantly to this mode.



**TABLE 3**

**CCs between some significant PCs and physical parameters associated with NEM**

NEM parameter	PC1 (OND)	PC1 (Oct)	PC1 (Nov)	PC1 (Dec)	PC1 (Jan)	PC2 (OND)	PC2 (Nov)	PC2 (Jan)	PC3 (Oct)
NEM onset	-0.33*	-0.56**				0.07			0.23*
NEM w/d	0.18#			0.20*	0.40*			0.34*	
SOI(Oct)	-0.44**	-0.06				0.18#			0.18#
STR(Oct)	-0.44**	-0.15				0.35*			0.48**
STR(Nov)			0.30*				0.27*		
CD days (Nov)			-0.03				0.21*		
STR(Dec)				0.36**					
STR(Jan)					0.24#			-0.09	
SOI(Jan)					0.21*			0.05	

\*\*,\*,# : significant at 1%, 5% and 10% level respectively;  
 PC : Principal Component,  
 NEM onset : Date of northeast monsoon onset,  
 NEM w/d : Date of northeast monsoon withdrawal,  
 SOI : Southern Oscillation Index,  
 STR : latitudinal location of Sub Tropical Ridge at 200 hPa over 78°E,  
 Cddays : No. of days of cyclones and depressions, OND : as in Table 1(a)  
 (NEM onset / withdrawal data : based on 1901-2004, SOI data : 1901-2006, STR data : 1951-2006, CDdays data : 1901-2006)

**TABLE 4**

**Conditional means of elements of PC2 (OND) and PC3 (Oct) for various intervals of SOI (Oct)**

SOI (Oct) interval	PC2 (OND)		PC3 (Oct)	
	N	Mean (cm)	N	Mean (cm)
<-10	20	-5.8	20	-1.9
-10 to -5	12	-2.6	16	-1.7
-5 to 0	23	-1.0	19	-0.3
0 to 5	17	4.5	17	-0.4
5 to 10	19	2.5	19	1.1
>10	13	9.5	13	7.5

N:Sample size; SOI & PC: As in Table 3

The PC1 (OND) being the most dominant empirical mode is likely to be associated with the overall strength of NEM. In Figs. [2(i)b-e] we present the mean pattern of RFA composites over the 9 sub-regions for the years when PC1 is deviated by 1 SD (35.0 cm) along with the low level (850 hPa) composited wind anomalies over the NEM region during the period 1950-2006 using NCEP monthly composite datasets. Easterly (westerly) anomalies are seen during 7 (8) years when  $PC1 \geq 1SD$  ( $PC1 \leq -1SD$ ) indicating prevalence of strong (weak) easterlies over the NEM region. The mean composited RFAs over all the

sub-regions except NCAP are highly positive during 16 years when  $PC1 \geq 1SD$  and negative during 19 years when  $PC1 \leq -1SD$  which when corroborated with the wind anomalies implies that PC1 is associated with easterly strength over the NEM region which is representative of the overall NEM strength.

The PC1 (OND) being the most dominant empirical mode is likely to be associated with the overall strength of NEM. In Figs. [2(i)b-e] we present the mean pattern of RFA composites over the 9 sub-regions for the years when

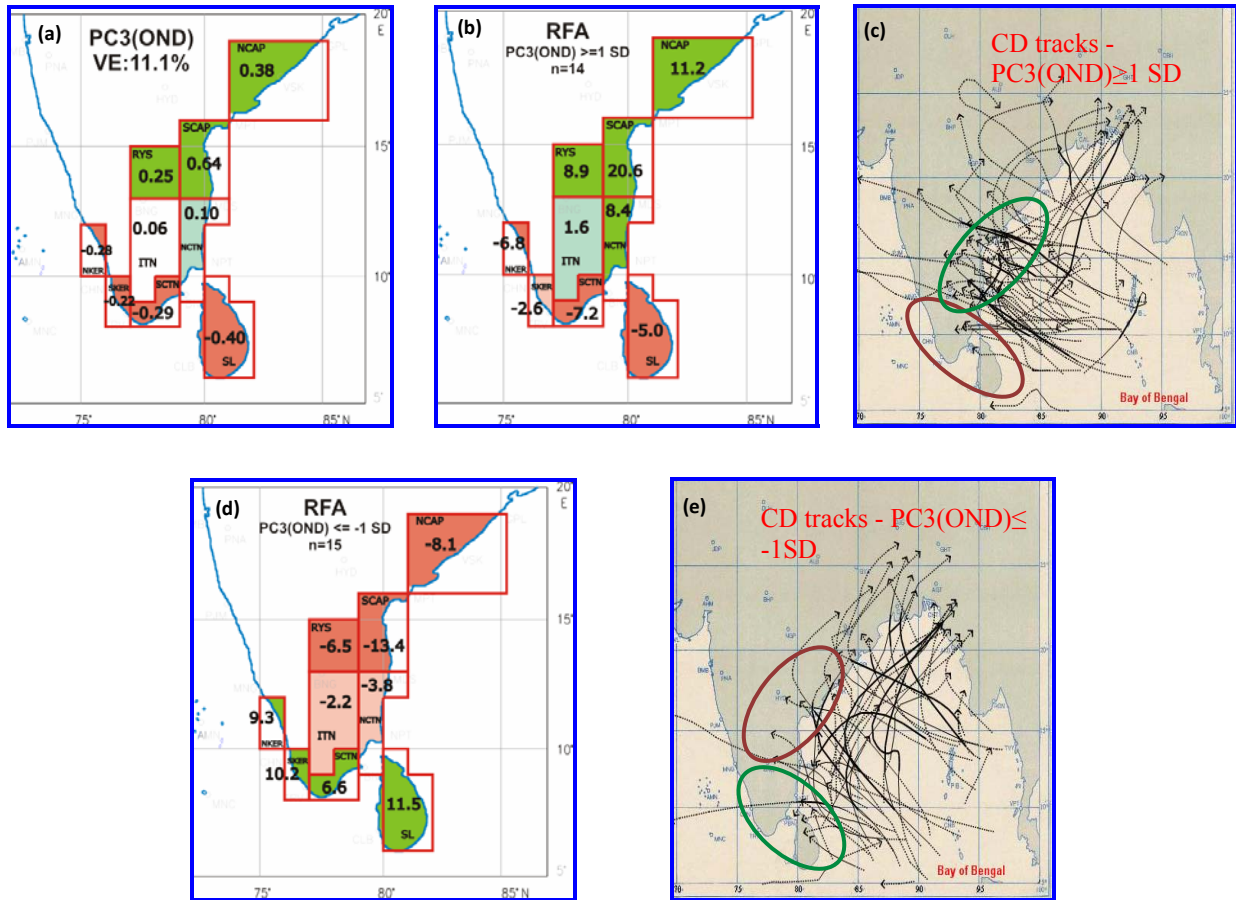


**Fig. 2(iii) (a-e).** (a) Spatial loadings of PC3(OND), (b&d) mean composited RFA(OND) (in cm) over the 9 sub-regions and (c&e) tracks of C&Ds over BOB region in OND during years when PC3(OND) deviated by 1 SD of PC3(OND) [RFA, n & colour codes : as in Fig. 2(i)]

PC1 is deviated by 1 SD (35.0 cm) along with the low level (850 hPa) composited wind anomalies over the NEM region during the period 1950-2006 using NCEP monthly composite datasets. Easterly (westerly) anomalies are seen during 7-8 years when  $PC1 \geq 1SD$  ( $PC1 \leq -1SD$ ) indicating prevalence of strong (weak) easterlies over the NEM region. The mean composited RFAs over all the sub-regions except NCAP are highly positive during 16 years when  $PC1 \geq 1SD$  and negative during 19 years when  $PC1 \leq -1SD$  which when corroborated with the wind anomalies implies that PC1 is associated with easterly strength over the NEM region which is representative of the overall NEM strength.

To further substantiate the link between the empirical and the physical modes of PC1, relation between PC1 and the following physical features known to be associated with NEM performance is analysed using correlation and CM analysis: (i) Temporal extent of NEM season, represented by its dates of onset / withdrawal over

CTN (ii) SOI (Oct), shown to be negatively correlated with the NEM activity (Raj and Geetha, 2008) and (iii) STR(Oct) at 200 hPa over the Indian region [Raj *et al.* (2004) and Raj & Geetha (2008)], also shown to be associated with NEM activity. The results are presented in Tables (3&4).

The CCs between PC1, which explains 54.8% variance and the above time series are given in Table 3. The CCs with the dates of onset and withdrawal are - 0.33 (5% LS) and 0.18 (10% LS) implying that positive (negative) PC1 is associated with early (late) onset and late (early) withdrawal. Also, the CCs between PC1 and SOI (Oct) / STR (Oct) are -0.44 (both) (1% LS) implying that positive (negative) PC1 is associated with negative (positive) SOI (Oct) and southward (northward) location of STR (Oct). These results are consistent with the known relation between SOI (Oct) / STR (Oct) and the NEM activity and lend further support to the postulate that PC1 (OND) represents the overall regional NEM strength.

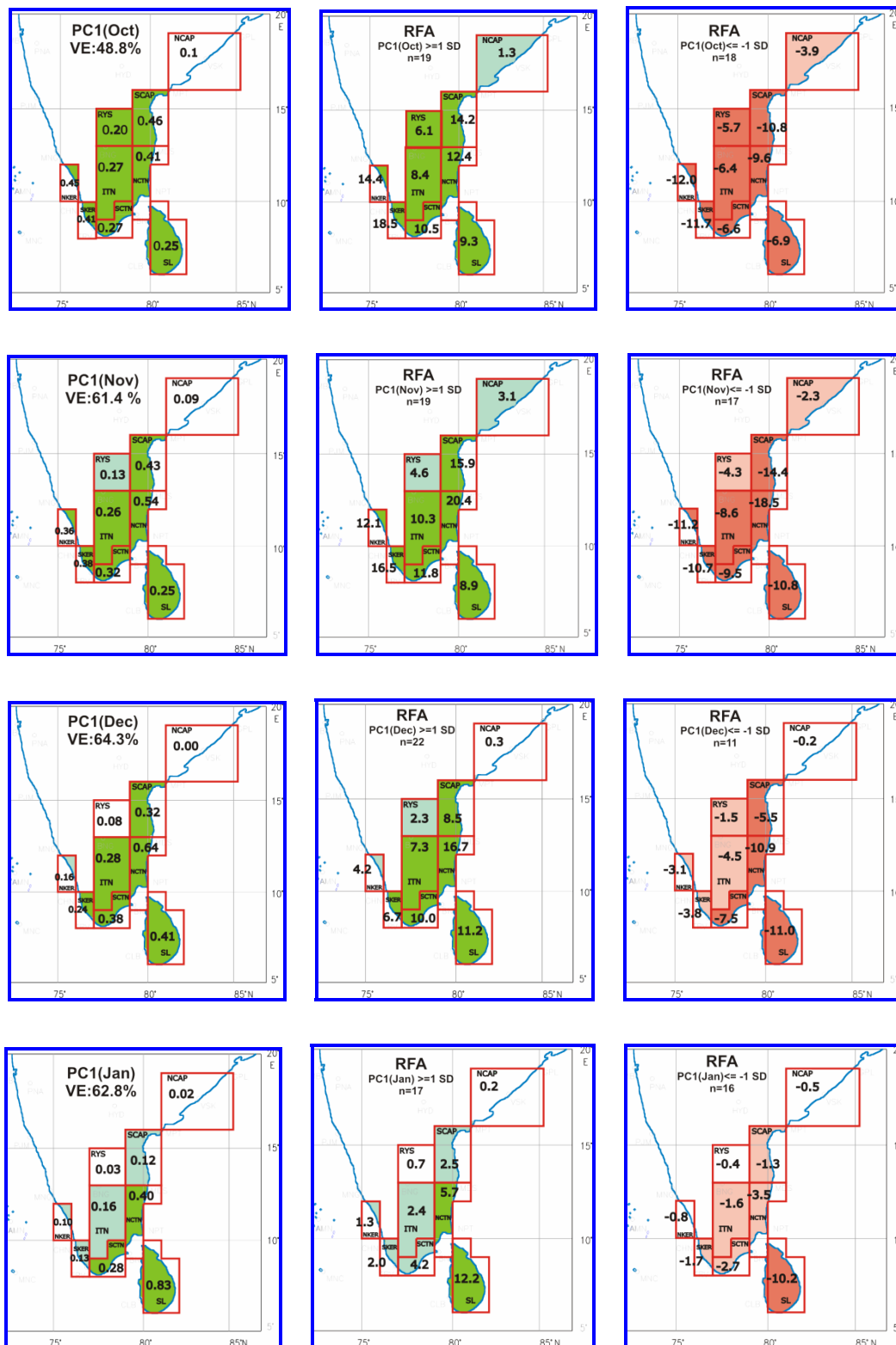
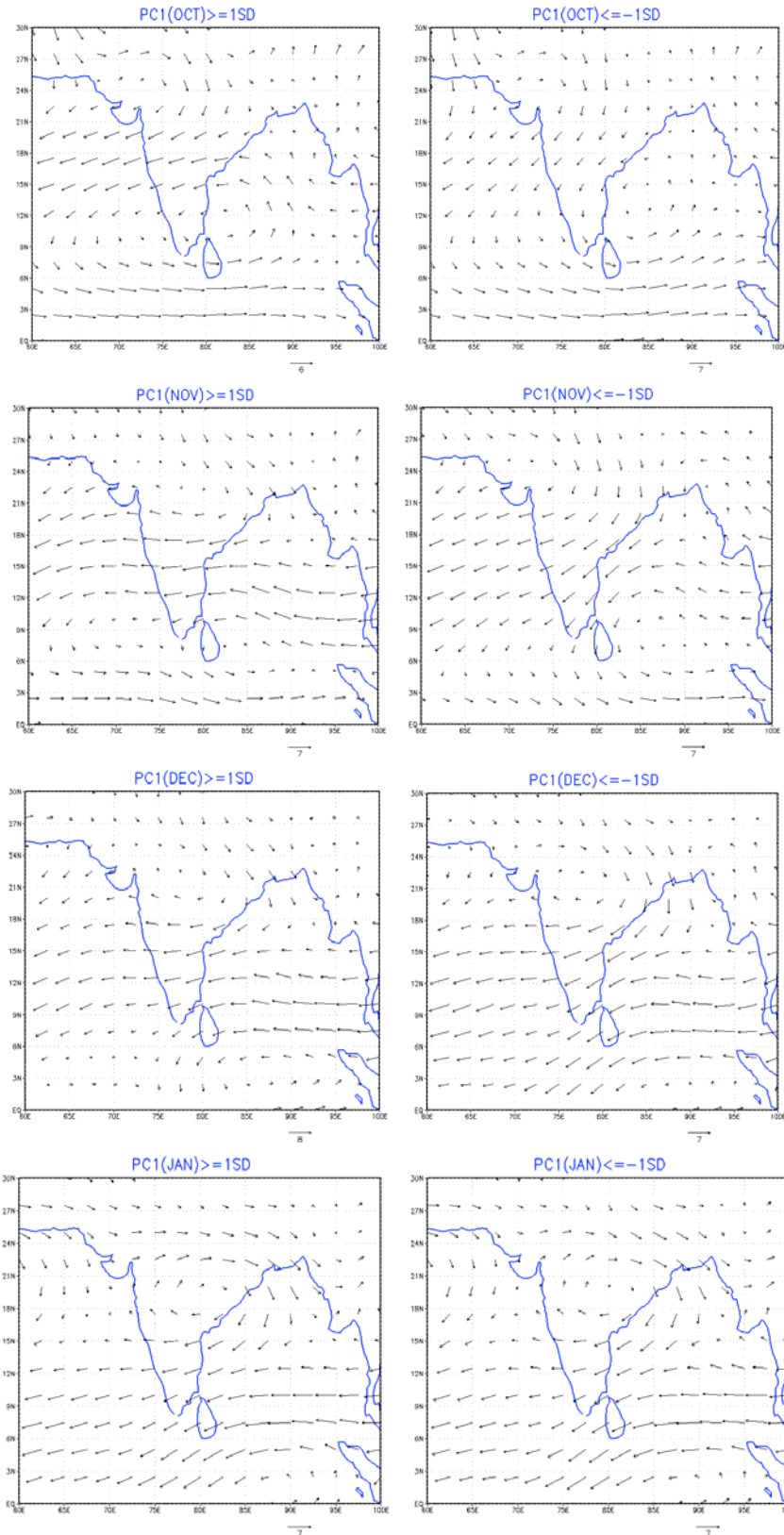
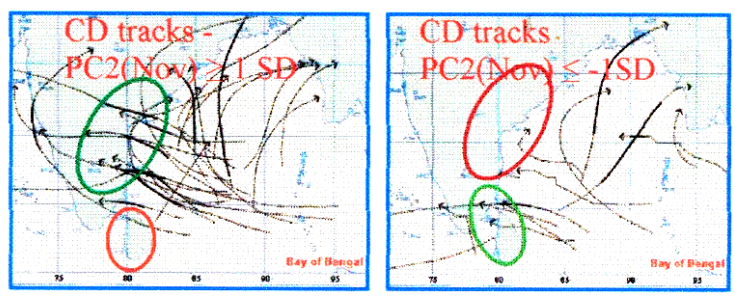
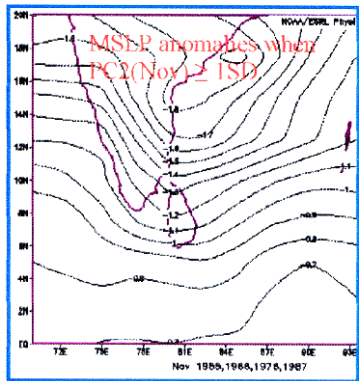
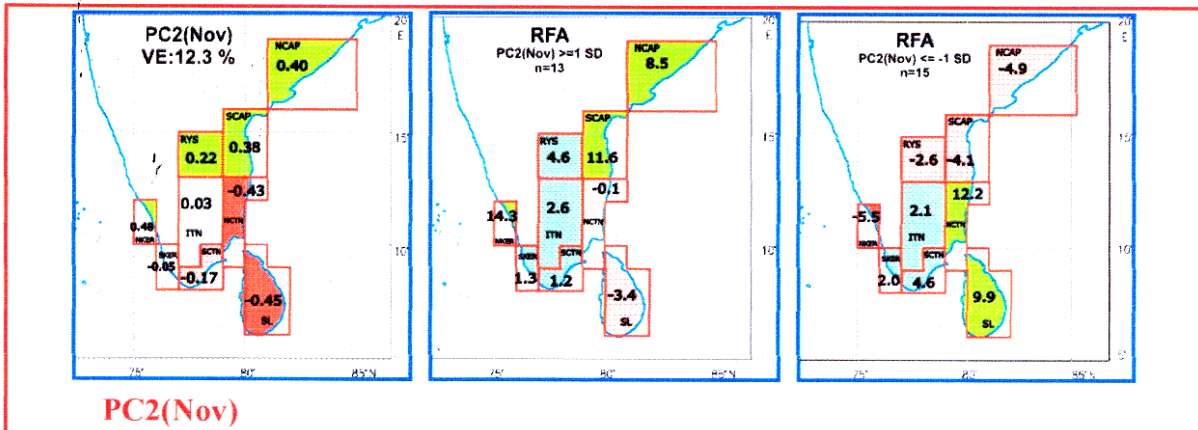
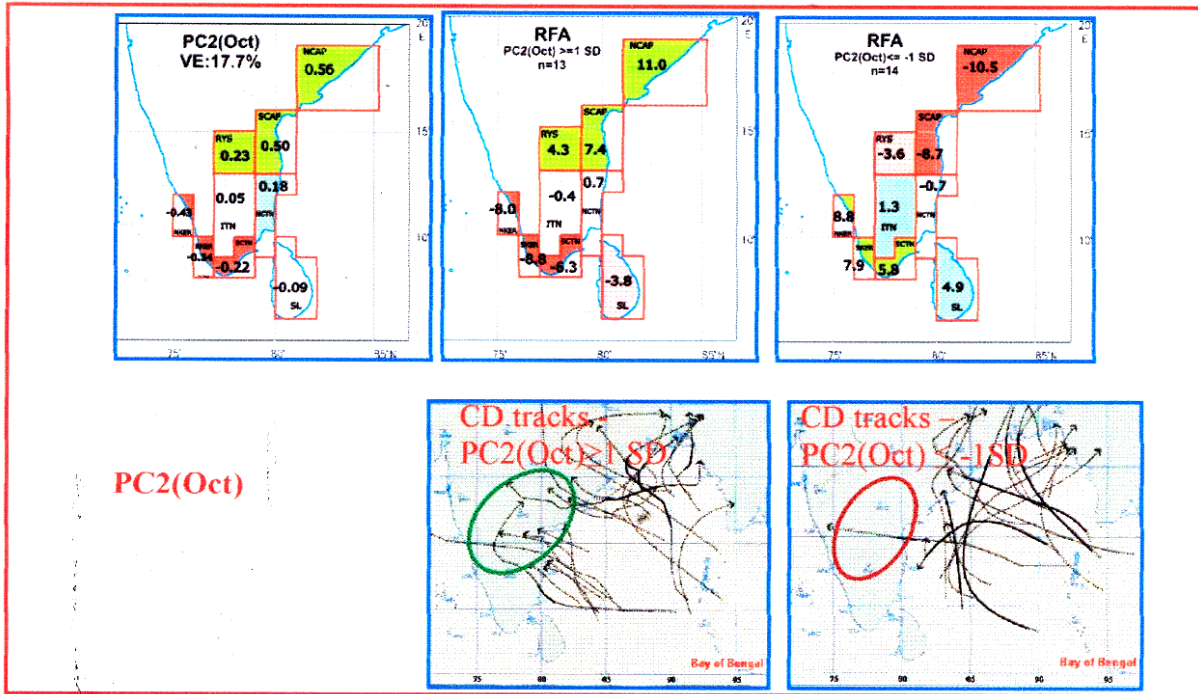


Fig. 3[i (a)]. Monthly spatial loadings of PC1 and mean RFAs (corresponding to concerned months in cm) over the 9 sub-regions during years when PC1 (Oct), PC1 (Nov), PC1 (Dec) and PC1 (Jan) deviated by the respective SDs [RFA, n & colour codes: as in Fig. 2(i)]



**Figs. 3[i] (b).** 850 hPa wind composites during years when PC1(Oct/Nov/Dec/Jan)  $\geq$  1SD & PC1(Oct/Nov/Dec/Jan)  $\leq$  -1SD (Source : NCEP reanalysis datasets, 1950-2006)





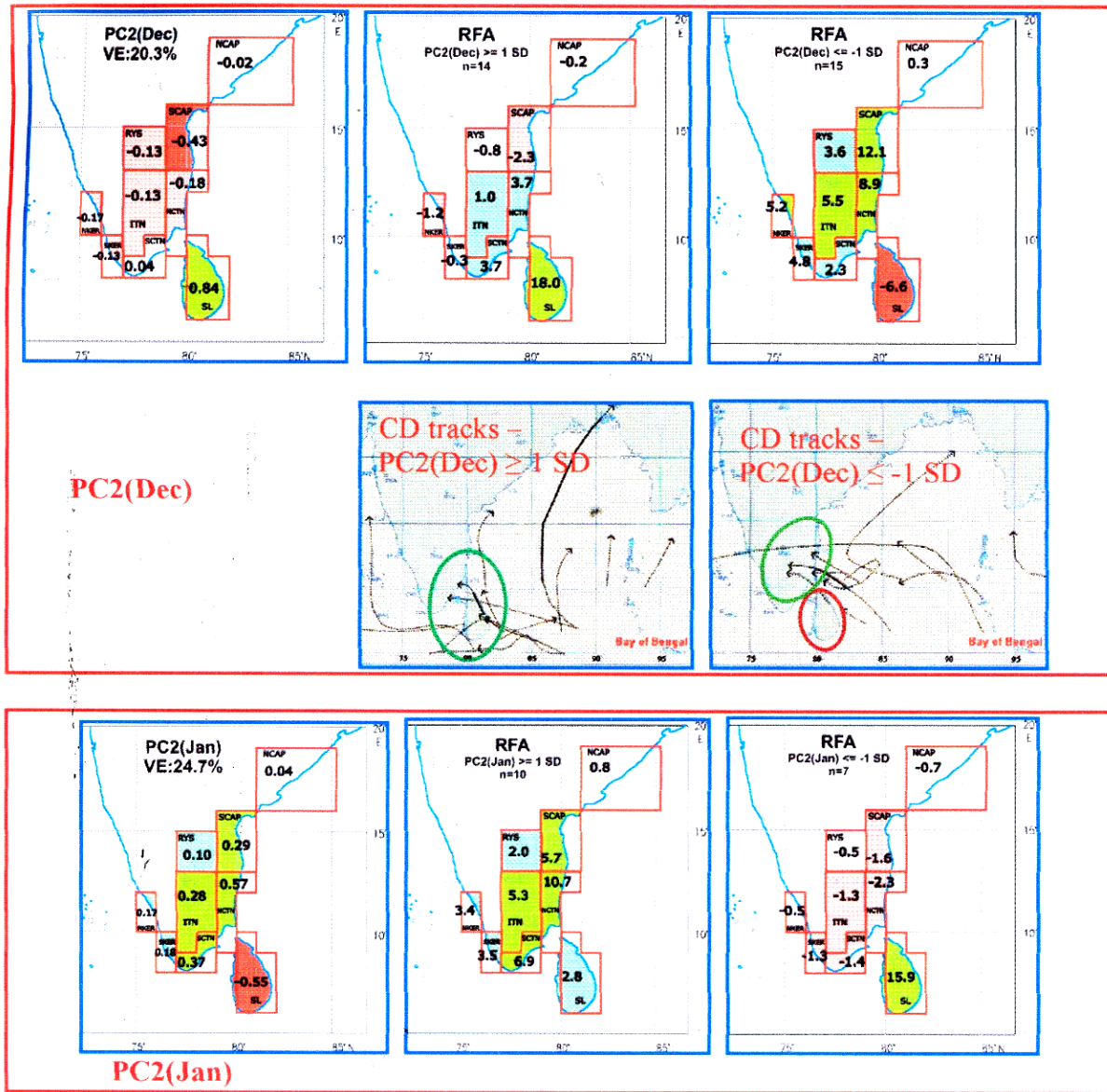
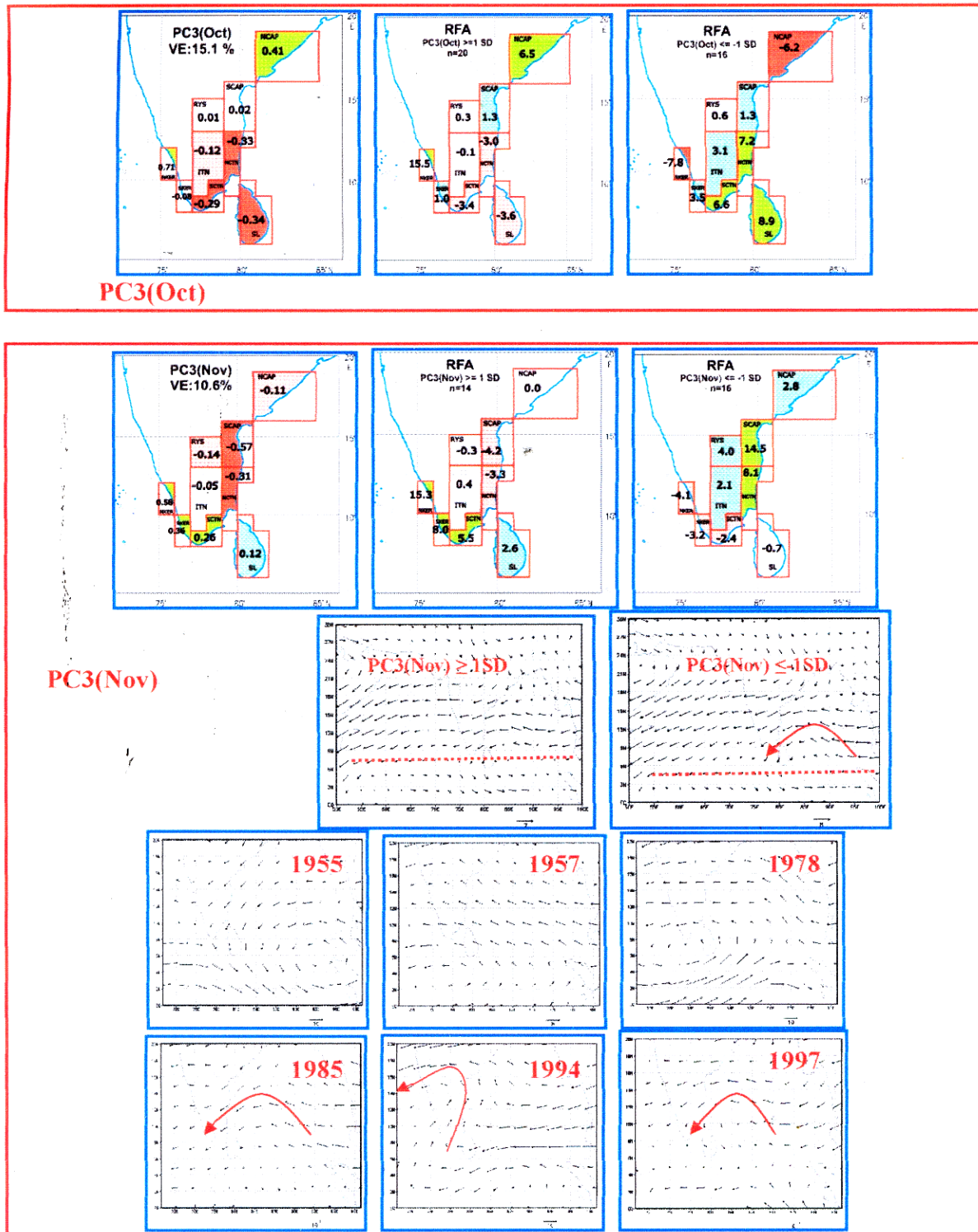


Fig. 3(ii). Spatial loadings of PC2(Oct/Nov/Dec/Jan) along with composited mean RFAs (corresponding to concerned months in cm) over the 9 sub-regions and composited tracks of C & Ds over BOB region during Oct/Nov/Dec during years when PC2 deviated by ±1 SD. For the month of November, NCEP monthly composites of MSLP in hPa during years with PC2(Nov) ≥ 1 SD during the period 1950-2006 are also shown. [RFA, n & colour codes: as in Fig. 2(i)]

The PC2 mode explains 15.1% variance in the dataset. The mean composited RFAs during 19 and 18 years respectively when  $PC2 \geq 1SD$  and  $PC2 \leq -1SD$  ( $SD=18.5cm$ ) are depicted in Figs. [2(ii)b-e]. The RFAs for NKER and SL are 27cm and -9.8 cm respectively when  $PC2 \geq 1SD$ , but, -13.4cm and 21.5 cm respectively when  $PC2 \leq -1SD$ . To bring out the physical features associated with this mode, we present the CCs between PC2 and SOI (Oct) /STR (Oct) (Table 3) and CMs of PC2 for various intervals of SOI (Oct) (Table 4). As shown,

PC2 is modestly positively correlated with SOI (Oct) ( $CC = 0.18$ , 10% LS) and significantly positively related to STR (Oct) ( $CC = 0.35$ , 5% LS). The profile of CMs of PC2 which progressively increases from -6 when SOI (Oct) < -10 to 10 when SOI (Oct) > +10 clearly brings out the existence of positive relation between the two variables. Thus, positive anomaly of PC2 is associated with positive SOI (Oct) and northward location of STR(Oct) which in turn are associated with good SWM activity (Raj *et al.*, 2004). The pattern of PC2 loadings



**Fig. 3(iii).** Spatial loadings of PC3(Oct/Nov) along with the composited mean RFAs (corresponding to concerned months in cm) over the 9 sub-regions in Oct/Nov during years when PC3(Oct/Nov) deviated by 1 SD. Composited mean flow pattern at 850 hPa and the latitudinal location of equatorial trough during years when PC3(Nov)  $\geq \pm 1SD$  during the period 1950-2006 with illustrations [RFA, n & colour codes: as in Fig. 2(i)]

being strongly positive over NKER and negative over CTN and SL is consistent with the known pattern of good SWM rainfall over NKER and poor rainfall over CTN associated with SWM during October. Thus, PC2 appears to represent the SWM rainfall realised during October prior to the onset of NEM which breaks in during the second half of the month.

The PC3 mode explains 11.1% variance in the dataset. The mean composited RFAs of the sub-regions during 14 years when  $PC3 \geq 1SD$  and 15 years when  $PC3 \leq -1SD$  ( $SD = 16.0$  cm) are shown in Figs. [2(iii)b-e] along with the tracks of CDs during those years. The mean RFA are positive over SCAP, NCAP, RYS and NCTN which have positive loadings and are negative over SL, SCTN, NKER and SKER with negative loadings. During years when  $PC3 \geq 1SD$ , large number of CDs have crossed the southern peninsular coast especially CAP and traversed over RYS. When  $PC3 \leq -1SD$ , the CDs have mostly recurred towards northeast with only a few crossing the extreme south peninsula and the SL coast. The PC3 mode is thus shown to be associated with the passage of CDs over the NEM area during OND.

The inferences from the above PCA for OND rainfall of 9 sub-regions and the analysis carried out to ascribe physical reasoning to the first three dominant modes could be stated as follows: The first empirical mode PC1 ( $VE = 54.8\%$ ) with all positive loadings is associated with the overall NEM strength and is related well with several dominant global and regional features which have been shown to be strongly associated with Indian NEM. The second mode, PC2 ( $VE = 15.1\%$ ) is associated with extended SWM during October, prior to the onset of NEM. The third mode, PC3 ( $VE = 11.1\%$ ), appears to represent the rainfall associated with the passage of CDs over the NEM area. These three modes together describe 81% of the total variance in the spatial rainfall distribution during the NEM season.

Taking into consideration, the intra-seasonal variation of NEM rainfall, it is important to analyse the rainfall patterns on monthly scales too. As such, we next conduct EOF analysis on the monthly rainfall series of October, November, December and the subsequent January of the 9 sub-regions for the period 1900-2006.

### 3.3.2. PCA in monthly scales

PCA of monthly rainfall of October-January is conducted similar to the analysis on the seasonal scale. Three PCs are retained for the months of October and November, and two PCs are retained for December and January based on the Kaiser-Guttman test of significance

of PCs. Identification of physical modes associated with each significant PC is substantiated through CCs, CMs presented in Tables (3&4) and pattern matching maps presented in Figs. [3(i-iii)].

#### 3.3.2.1. PC1 of October, November, December and January

The variances explained by PC1 of October, November, December and January are 48.8%, 61.4%, 64.3% and 62.8% respectively. Fig. [3(i)a] present their spatial loadings and the RFAs over the 9 sub-regions during years when PC1 (Oct), PC1 (Nov), PC1 (Dec) and PC1 (Jan) are deviated by more than the corresponding SDs of 19.9 cm, 23.7 cm, 16.6 cm and 9.2 cm respectively. As seen, the loadings are positive over all the sub-regions except NCAP wherein they are almost insignificant and the mean RFAs over all the sub-regions are positive when  $PC1 \geq 1SD$  and negative when  $PC1 \leq -1SD$  for all the four months. The values of RFA (both positive and negative) over NCAP are very small / negligible when compared to those over other sub-regions indicating that this sub-region is not very much influenced by this dominant mode. For RYS, a strongly positive loading in October becomes modestly positive in November which becomes insignificant for the later months of December and January. Towards the fag end of the season, contributions are mainly from NCTN, SCTN and SL. During December/January, contributions from SL to this mode increase substantially and that from NKER, SKER, ITN and SCAP decrease as revealed by the RFA distribution. This pattern of spatial and temporal variability in PC1 on monthly scale ties in well with the climatology of NEM rainfall. The low level (850 hPa) wind composites over the NEM region for the years when  $PC1$  (Oct/Nov/Dec/Jan)  $\geq 1SD$  and when  $PC1$  (Oct/Nov/Dec/Jan)  $\leq -1SD$  during the period 1950-2006 determined using NCEP monthly composite datasets are presented in Fig. [3(i)b]. Over the NEM region, strong zonal easterlies are associated with  $PC1 \geq 1SD$  indicating good NEM activity but dominant northerly meridional winds are associated with  $PC1 \leq -1SD$  indicating weak NEM activity. The RFA patterns and the low level wind flow patterns suggest that this mode is associated with the overall NEM strength during all the four months of October-January.

This link between the empirical and physical modes is further substantiated by the following results presented in Table 3. The CC between PC1 (Oct) and date of onset of NEM is -0.56 (1% LS) which implies that early/late onset of NEM is associated with positive/negative anomalies of PC1 (Oct). However, the strong negative association of SOI (Oct) and STR (Oct) with the PC1 (OND) is not reflected in the case of PC1 (Oct). This may



be due to the fact that during October the dominant seasonal circulation pattern over the southern peninsular India undergoes transition from SWM features during the first half to NEM features in the second half. PC1 (Nov) is positively related to STR (Nov) (CC = 0.30, 5% LS). PC1 (Dec) is positively related to NEM withdrawal dates (CC = 0.20, 5% LS) and STR (Dec) (CC = 0.36, 1% LS). PC1 (Jan) is positively related to NEM withdrawal dates (CC = 0.40, 5% LS), STR (Jan) (CC = 0.24, 10% LS) and SOI (Jan) (CC = 0.21). These results are in tune with the changing nature of relationship between SOI / latitudinal location of STR at 200 hPa level and NEM rainfall with the advancement of the season. As SOI and latitudinal location of STR200 influence the two monsoons in opposite fashion, the relation for the entire month of October becomes insignificant. The variance explained by PC1, is less for October (48.8%) than for the other months (> 60%) and the OND season (54.8%) which could also be due to the mixed types of rainfall realised during October.

### 3.3.2.2. *PC2 of October, November, December and January*

The second dominant mode PC2 for October, November and December explains 17.7%, 12.3% and 20.3% variance respectively. This mode is shown to be linked to the rainfall associated with the passage of CDs for all the three months as detailed below. Fig. [3(ii)] presents the loadings associated with PC2, RFA composites during years when  $PC2 \geq \pm 1$  SD of PC2 of the respective month and also composited tracks of CDs over the BOB during the corresponding two sets of years for the months of October, November and December.

*PC2 (Oct)* : This mode explains 17.7% variance and the loadings are positive for NCAP, SCAP and RYS; negative for NKER, SKER, SCTN and SL. The RFAs are positive over the former sub-regions and negative over the latter when  $PC2$  (Oct)  $\geq 1$ SD (12.0 cm) (13 years). Opposite sign pattern is realised when  $PC2$  (Oct)  $\leq -1$ SD (14 years). Generally, during October, most of the CDs forming over the BOB, make landfall over east coast of India north of 15° N and so do not substantially affect the regions of south CTN, Kerala and Sri Lanka. During the years when  $PC2$  (Oct)  $\geq 1$ SD, the former sub-regions have been affected by passage of CDs over these areas and hence have received good rainfall. During the years with  $PC2$  (Oct)  $\leq -1$ SD, most of the CDs forming over BOB have recurved towards northeast and those crossing CAP have been meagre leading to negative RFA over these sub-regions [Fig. 3(ii)].

*PC2 (Nov)* : This mode explains 12.3% variance. The loadings are positive over NCAP, SCAP, NKER and

RYS. They are strongly negative over NCTN and SL, negative over SCTN, insignificant over ITN and SKER. The RFAs for the 13 years when  $PC2 \geq 1$ SD and for the 15 years when  $PC2 \leq -1$ SD (SD = 10.6 cm) also reiterate the pattern generated by the loadings. The composited tracks of CDs over BOB for the corresponding sets of years depict the region influenced by the CDs during the respective years. When  $PC2$  (Nov)  $\geq 1$ SD, the northern sub-regions get influenced by the passage of CDs and must have benefitted from the associated rainfall. When the  $PC2$  (Nov)  $\leq -1$ SD, the cyclonic activity over the BOB has been poor and hence associated with negative RFAs.

That the passage of CDs and the associated rainfall is likely to be the physical mode associated with PC2 (Nov) is further substantiated as follows: (a) The CC between PC2 (Nov) and the number of CD days over NIO is positive (0.21, 5% LS) (Table 3), (b) NCEP reanalysis composite of MSLP anomalies in November during 4 years of the period 1950-2006 when  $PC2$  (Nov)  $\geq 1$ SD presented in Fig. [3(ii)] shows that the anomalies are negative over most parts of southern peninsula, reaching the lowest value of -1.8 hPa over 13° N. The MSLP anomaly pattern further supports the strong influence of greater cyclonic activity over northern latitudes which is manifested in PC2 (Nov). When  $PC2$  (Nov)  $\leq -1$ SD, there are less number of CDs over BOB but most of them crossed the coast south of 10° N, some dissipated in the sea and the remaining recurved northwards. It is well known from the NEM climatology that when CDs cross the east coast of southern India, the chief rainfall belt associated with the crossing extends far more to the north than to the south (IMD, 1973). This explains the substantially positive RFAs over the NCTN (12.2 cm) when  $PC2$  (Nov)  $\leq -1$ SD.

*PC2 (Dec)* : PC2 (Dec), explaining 20.3% variance is a very interesting mode with strong, lone positive loading for the SL sub-region and negative loadings for most of the other regions with SCAP having the highest absolute value [Fig. 3(ii)]. During the month of December, generally, formation and movement of CDs are confined to south of 10°N latitude influencing south TN and Sri Lanka. During the 14 years when  $PC2$  (Dec)  $\geq 1$ SD (SD = 10.0 cm), the sub-region of SL is the major beneficiary (RFA = 18 cm) and most of the CDs forming over BOB have crossed SL coast and traversed over SL, not affecting the Indian NEM region. During the 15 years when  $PC2$  (Dec)  $\leq -1$ SD, most of the CDs over the BOB have crossed and traversed over the southern Indian peninsula and the RFAs over the sub-regions of India are positive and RFA over SL is negative.

*PC2 (Jan)* : The second dominant mode of January, PC2 (Jan), explaining 24.7% variance, has a negative

loading for SL but positive loadings for all the sub-regions of peninsular India as shown in Fig. [3(ii)]. The RFAs over the nine sub-regions during the 10 / 7 years when  $PC2(\text{Jan}) \geq 1SD$  and  $PC2(\text{Jan}) \leq -1SD$  ( $SD = 5.8$  cm) are also presented in Fig. [3(ii)]. During the former years when  $PC2(\text{Jan}) \geq 1SD$ , the RFAs over all the sub-regions are positive, strongly over NCTN. During the latter years, when  $PC2(\text{Jan}) \leq -1SD$ , the RFAs over the Indian sub-regions are negative and that over SL is strongly positive. Thus,  $PC2(\text{Jan})$  could be associated with a situation when RFAs over the Indian sub-regions and SL are of opposite sign. As the January rainfall of SL is significantly positively related to that of several Indian sub-regions [CCs : NCTN (0.41), SCTN (0.42) and ITN (0.32) : 0.1% LS (Table 2)], such incidences could occur only occasionally.

### 3.3.2.3. *PC3 of October and November*

*PC3 (Oct):*  $PC3(\text{Oct})$  explains 15.1% variance of October rainfall, and has positive loadings for the sub-regions of NKER and NCAP and negative loadings for SL, NCTN and SCTN [Fig. 3(iii)]. The other sub-regions do not contribute much to this mode. The RFAs for  $PC3(\text{Oct}) \geq 1SD$  ( $SD = 11.0$  cm; 20 years) and  $PC3(\text{Oct}) \leq -1SD$  (16 years), presented in Fig. 4(iii) also clearly show this pattern of rainfall variation. During October, normally, good rainfall over NKER and NCAP and deficient rainfall over CTN and SL are associated with extended SWM season.

From Table 3, it is seen that  $PC3(\text{Oct})$  is positively related to onset dates of NEM (CC: 0.23, 5% LS), SOI (CC: 0.18, 10% LS) and STR200 (Oct) (CC: 0.48, 1% LS). The CM analysis of  $PC3(\text{Oct})$  for various intervals of SOI (Oct), presented in Table 4, clearly brings out the modest positive relationship between  $PC3(\text{Oct})$  and SOI (Oct). It is worthwhile to note that onset dates of NEM which is strongly negatively related to  $PC1$  is positively related to  $PC3$ , *i.e.*, early (late) onset associated with negative (positive) values of  $PC3$  in a modest way. Thus  $PC3(\text{Oct})$  is associated with SWM contribution during October prior to the onset of NEM. That NKER and NCAP (NCTN and SCTN) are strongly positively (negatively) associated with this mode tie in well with the climatological fact that these sub-regions are generally benefitted well from the SWM (NEM) rather than the NEM (SWM).

*PC3 (Nov):* For  $PC3(\text{Nov})$  which explains 10.6% variance, the loadings are positive over the southern sub-regions of SCTN, SKER and NKER and to some extent SL also, but negative over the northern sub-regions of NCTN, SCAP and to some extent RYS and NCAP [Fig. 3(iii)]. The RFAs presented for the

14 / 16 years when  $PC3(\text{Nov}) \geq 1SD$  and  $PC3(\text{Nov}) \leq -1SD$  ( $SD = 9.9$  cm) also bring out the spatial variation clearly.

The mode  $PC3$  is shown to be related to the influence of STR200 and the equatorial trough at 850 hPa level over the Indian region (ET850) on NEM rainfall as shown in the following analysis. The 850 hPa wind composites during the period 1950-2006 when  $PC3(\text{Nov}) \geq \leq \pm 1SD$  are presented in Fig. 4(iii). During 5 years when  $PC3(\text{Nov}) \geq 1SD$ , the mean latitudinal location of the ET850 over the Indian region is along 7-8° N and rainfall activity prevailed over the southern sub-regions of SCTN, SKER, NKER and SL. Rainfall over SCAP and NCTN has been sparse. During 10 years when  $PC3(\text{Nov}) \leq -1SD$ , the ET850 over the Indian region is located along 5° N about 2-3° further southwards in which case, NEM should be weak over the entire peninsula especially the northern parts. But the positive contribution from the sub-regions of SCAP, NCTN and RYS when  $PC3(\text{Nov}) \leq -1SD$  is interesting. In this context, the role of yet another important synoptic scale feature associated with the location of ET850, *viz.*, the formation and passage of easterly waves close to ET is relevant. The 850 hPa mean wind flow pattern in the second case also indicates a wave like flow with southerly and northerly wind components off the southeastern coast of India. Passage of easterly waves over southern peninsular India when the equatorial trough moves south of 8°N has been observed as a synoptic feature associated with NEM activity (IMD, 1973). Illustrations depicting the wave like perturbations in the easterly flow during 3 years (1985, 1994 and 1997) when  $PC3(\text{Nov}) \leq -1SD$  and 3 other years when  $PC3(\text{Nov}) \geq 1SD$  (*viz.*, 1955, 1957 and 1978) and no such feature is evident are also presented in Fig. 4 (iii). Thus, passage of easterly waves over slightly northern latitudes could explain the cause for positive RFAs over SCAP, NCTN and RYS and subdued rainfall activity over SL when  $PC3(\text{Nov}) \leq -1SD$  and ET is located southwards.

### 3.4. *Remarks*

Several relations and tele connections corresponding to NEM of Tamil Nadu derived in earlier works have held good for the NEM signal prised from the rainfall series of the nine regions through PCA as represented by the first and most dominant PC. This has shown that despite diversity, there is considerable homogeneity in the NEM rainfall series of the sub-regions considered.

It must be added here with abundant caution, that the physical features associated with the PCs, identified in this

study, are unlikely to constitute an exhaustive list. There may be other physical features not identified in this study, but related or even better related to the various PCs. Such unidentified features are unlikely to be unrelated to the identified features, in as much as meteorological parameters representing the physical features of a region are always likely to be inter related to some extent displaying multi-collinearity. The physical features that we have identified as representing the various empirical modes are consistent with established relations, easy to interpret and understand. That the list is not exhaustive, offers scope to pursue this study still further.

#### 4. Conclusion

The region of southern peninsular India benefitted by northeast monsoon and Sri Lanka are divided into 9 sub-regions and subjected to EOF analysis in seasonal and monthly scales to determine spatial patterns in the NEM rainfall variability. Physical modes associated with significant empirical modes are identified using correlation, conditional mean and composite analysis. The following are the important conclusions arrived at:

(i) More than 80% of the variance in the dataset is explained by the first three PCs in the case of OND, October and November and by the first two PCs in the case of December and January. The PC1 of the respective month / season explains about 50-65% and the remaining significant PCs about 25% of the spatial rainfall variation. In all the cases, PC1 is identified as the overall NEM strength.

(ii) PC1 (Oct) is negatively correlated with date of onset of NEM and PC1 (Dec) is positively related to date of withdrawal of NEM which substantiate the physical link between the PC1 and the overall NEM activity.

(iii) Changing nature of relationship between NEM rainfall of Tamil Nadu and SOI / STR at 200 hPa level, from the first to the second half of NEM season is reiterated in this study. PC1 (Oct) is modestly negatively related to latitudinal position of STR (Oct), but, PC1 (November/December/January) are positively related to STR (Nov/Dec/Jan). Further, PC1 (OND) is negatively related to SOI (Oct) but PC1 (Jan) is positively related to SOI (Jan).

(iv) Contrasting nature of relationship between SOI / STR with SWM and NEM are also brought out clearly. PC2 (OND) and PC3 (Oct) each explaining 15% of rainfall variability are identified with SWM contribution prior to the onset of NEM during October. With STR (Oct), PC1 (OND) representing NEM is negatively related

whereas PC2 (OND) representing SWM is positively related.

(v) Another important physical mode identified is the rainfall associated with the passage of cyclones and depressions, which is related to PC3 (OND) explaining about 10% of variability in OND rainfall. For the individual months, the mode is related to PC2 (Oct/Nov/Dec) which explains 10-20% variability.

(vi) There is little contribution from PC1 representing overall NEM strength to the sub-region of NCAP. The variability in rainfall over NCAP results mainly from the rainfall associated with SWM activity during October (PC3) and passage of CDs during October and November (PC2).

(vii) An extended SWM season causes negative impact on the rainfall over NCTN and SCTN during October as revealed through the variation of PC3 (Oct).

(viii) During November, CDs crossing CAP lead to decrease of rainfall over NCTN, SCTN and SL as shown by the variation of PC3 (Nov). The PC3 (Nov) is shown to have an intricate relationship with latitudinal location of equatorial trough at 850 hPa and passage of easterly waves over peninsular India which are two important synoptic features having bearing on the NEM rainfall.

(ix) During December, passage of CDs, represented by PC2, increase rainfall over SL but, reduces the same over RYS.

#### Acknowledgement

The authors thank the referee for his detailed comments and critical remarks that helped to improve the manuscript. Thanks are also due to Shri N. Selvam, Regional Meteorological Centre, Chennai for his help in preparation of figures.

#### References

- Asnani, G. C., 2005, "Tropical Meteorology", 3, Ch 11 & 12, Prof. Asnani G. C., Pune, India.
- Bartzokas, A., Metaxas, D. A. and Ganas, I. S., 1994, "Spatial and temporal sea surface temperatures in the Mediterranean", *Int. J. Climatol.*, **14**, 201-213.
- Bedi, H. S. and Bindra, M. M. S., 1980, "Principal components of monsoon rainfall", *Tellus*, **32**, 296-298.
- Everson, R., Cornillon, P., Sirovich, L. and Webber, A., 1997, "An empirical eigen function analysis of SSTs in the western North Atlantic", *J. Phys. Oceanogr.*, **27**, 468-479.

- Guhathakurta, P., 2003, "Droughts in districts of India during the all India normal monsoon years and its probability of occurrence", *Mausam*, **54**, 2, 542-544.
- Geetha, B., 2012, "Indian northeast monsoon as a component of Asian winter monsoon and its relationship with large scale global and regional circulation features", Ph. D Thesis, University of Madras.
- India Meteorological Department, 1973(a), "Weather over the Indian seas during the post-monsoon season", FMU Report No.III-4.1.
- India Meteorological Department, 1973(b), "Northeast monsoon", FMU Report No. IV-18.4.
- India Meteorological Department, 2008a, "Cyclone eAtlas – IMD", Software on tracks of cyclones and depressions over North Indian Ocean during 1891- Current year.
- India Meteorological Department, 2008b, "CWCSTAT - A FORTRAN based software for generation of statistics on cyclones and depressions over the North Indian Ocean", Met. Monograph No. Climatology 23/2008.
- Krishnamurthy, E. V. and Sen, S. K., 1986, "Numerical algorithms – Computations in science and engineering", Ch-6, Affiliated East-West Press Ltd., New Delhi.
- Kondragunta, R. C., 2001, "On the intraseasonal variations of the Asiatic Summer monsoon", *Mausam*, **52**, 1, 217-226.
- Lorenz, E., 1956, "Empirical orthogonal functions and statistical weather prediction", Tech. Rep.1., Massachusetts Institute of Technology, USA.
- Mohapatra, M., Biswas, H. R. and Sawaisarje, G. K., 2011, "Spatial variability of daily rainfall over northeast India during summer monsoon season", *Mausam*, **62**, 2, 215-228.
- Nayagam, L. R., Janardanan, R. and Mohan, H. S. R., 2009, "Variability and teleconnectivity of northeast monsoon rainfall over India", *Global and Planetary Change*, **69**, 4, 225-231.
- Rao, Y. P., 1976, "Southwest monsoon", India Meteorological Department, Met. Monograph.
- Raj, Y. E. A., 2003, "Onset, withdrawal and intraseasonal variation of northeast monsoon over coastal Tamil Nadu, 1901-2000", *Mausam*, **54**, 3, 605-614.
- Raj, Y. E. A., Suresh, R., Sankaran, P. V. and Amudha, B., 2004, "Seasonal variation of 200 hPa upper tropospheric features over India in relation to performance of Indian southwest and northeast monsoons", *Mausam*, **55**, 2, 269-280.
- Raj, Y. E. A. and Geetha, B., 2008, "Relation between Southern Oscillation Index and Indian northeast monsoon as revealed in antecedent and concurrent modes", *Mausam*, **59**, 1, 15-34.
- Singh, C. V., 2004, "Empirical Orthogonal Function (EOF) analysis of monsoon rainfall and satellite-observed outgoing long-wave radiation for Indian monsoon: A comparative study", *Meteorology and Atmospheric Physics*, **85**, 4, 227-234.
- Srivastava, H. N. and Singh, S. S., 1993, "Empirical Orthogonal functions associated with parameters used in long range forecasting of Indian summer monsoon", *Mausam*, **44**, 1, 29-35.
- Wilks, 2010, "Statistical methods in the Atmospheric Sciences", 3rd ed., Academic Press, San Diego, USA.
- Yen, M. C. and Chen, T. C., 2000, "Seasonal variation of rainfall over Taiwan", *Int. J. Climatol.*, **20**, 803-809.
-